CO_2 Reforming of CH_4 on Ni(111): A Density Functional Theory Calculation

Sheng-Guang Wang,[†] Dong-Bo Cao,[†] Yong-Wang Li,[†] Jianguo Wang,[†] and Haijun Jiao*[,†,‡]

State Key Laboratory of Coal Conversion, Institute of Coal Chemistry, Chinese Academy of Sciences, Taiyuan, Shanxi 030001, P. R. China, and Leibniz-Institut für Katalyse e.V. an der Universität Rostock, Albert-Einstein-Strasse 29a, 18059 Rostock, Germany

Received: February 16, 2006; In Final Form: March 29, 2006

CO_2 reforming of CH_4 on Ni(111) was investigated by using density functional theory. On the basis of thermodynamic analyses, the first step is CH_4 sequential dissociation into surface CH ($CH_4 \rightarrow CH_3 \rightarrow CH_2 \rightarrow CH$) and hydrogen, and CO_2 dissociation into surface CO and O ($CO_2 \rightarrow CO + O$). The second step is CH oxygenation into CHO ($CH + O \rightarrow CHO$), which is more favored than dissociation into C and hydrogen ($CH \rightarrow C + H$). The third step is the dissociation of CHO into surface CO and H ($CHO \rightarrow CO + H$). This can explain the enhanced selectivity toward the formation of CO and H_2 on Ni catalysts. It is found that surface carbon formation by the Bouduard back reaction ($2CO = C_{(ads)} + CO_2$) is more favored than by CH_4 sequential dehydrogenation. The major problem of CO_2 reforming of CH_4 is the very strong CO adsorption on Ni(111), which results in the accumulation of CO on the surface and hinders the subsequent reactions and promotes carbon deposition. Therefore, promoting CO desorption should maintain the reactivity and stability of Ni catalysts. The computed energy barriers of the most favorable elementary reaction identify the CH_4 activation into CH_3 and H as the rate-determining step of CO_2 reforming of CH_4 on Ni(111), in agreement with the isotopic experimental results.

Introduction

The preparation of synthesis gas from natural gas, the most important step in the gas-to-liquid (GTL) transformation, has attracted increasing attention in the past decade.[1] Steam reforming (eq 1), partial oxidation (eq 2), and CO_2 reforming (eq 3) are the major processes for producing synthesis gas.

$$CH_4 + H_2O = CO + 3H_2 \qquad \Delta H^0_{298} = 206 \text{ kJ/mol} \tag{1}$$

$$CH_4 + {}^1/_2O_2 = CO + 2H_2 \qquad \Delta H^0_{298} = -36 \text{ kJ/mol} \tag{2}$$

$$CH_4 + CO_2 = 2CO + 2H_2 \qquad \Delta H^0_{298} = 247 \text{ kJ/mol} \tag{3}$$

Steam reforming is widely used today, but is expensive due to its endothermic nature and the requirement for low space velocities. In addition, the high H_2/CO ratio (3:1) is unsuitable for the synthesis of methanol or long-chain hydrocarbons in the Fischer−Tropsch synthesis.

In contrast to steam reforming, CH_4 partial oxidation is exothermic, but requires pure oxygen, which is produced in expensive air separation units and responsible for up to 40% of the cost of a synthesis gas plant.[2] In addition, this reaction is hazardous because of the hot spot (high-temperature gradient) in large-scale processes.

Although CO_2 reforming is endothermic, it produces synthesis gas with a lower H_2/CO ratio (1:1). Therefore, it is suitable for long-chain hydrocarbons in Fischer−Tropsch synthesis. Furthermore, it can be carried out with natural gas from fields containing a large amount of CO_2 without preseparation of CO_2 from the feed. CO_2 reforming of CH_4 may also provide a practical method for consuming the two greenhouse gases, CH_4 and CO_2.

Unfortunately, no industrial technology for CO_2 reforming of CH_4 has been developed yet, and no effective and economical catalysts are available. Many experimental and theoretical studies have been conducted on Ni-based catalysts,[3−24] which are more economical than noble metal catalysts. However, no detailed mechanism of Ni-catalyzed CO_2 reforming of CH_4 was proposed by using density functional theory calculations.

Many questions are still open for CO_2 reforming of CH_4. This reaction is strongly endothermic (247 kJ/mol) and disfavored thermodynamically, but experimental results indicated that Ni-catalyzed CO_2 reforming of CH_4 produces CO and H_2 in high selectivity and conversion rate. Experimental study found CHO and CH_2O as intermediates in the steam reforming systems on Ni-based catalysts, and both CH_x ($CH_4 \rightarrow CH_x \rightarrow C \rightarrow CO$)[25,26] and CH_xO ($CH_4 \rightarrow CH_x \rightarrow CH_xO \rightarrow CO$)[27−29] pathways were proposed. However, the key intermediates (CH_x or CH_xO species) and the main reaction pathways are still unclear.

In this paper, we present our calculations on all the possible intermediates in CO_2 reforming of CH_4 on Ni(111). Main intermediates were outlined and analyzed, and the energy barriers of the most favorable pathway were presented. This is a part of our work on detailed mechanism of Ni-catalyzed CO_2 reforming of CH_4.

Methods and Models

Density functional theory calculations within the generalized gradient approximation (GGA)[30] and the Perdew−Burke−Ernzerhof (PBE)[31] functional were carried out to calculate all the possible intermediates in CO_2 reforming of CH_4 on Ni(111). All calculations were carried out by using the Cambridge

* Corresponding author. E-mail: haijun.jiao@ifok-rostock.d.
† State Key Laboratory of Coal Conversion, Institute of Coal Chemistry.
‡ Leibniz-Institut für Katalyse e.V. an der Universität Rostock.

10.1021/jp060992g CCC: $33.50
Published on Web 05/03/2006

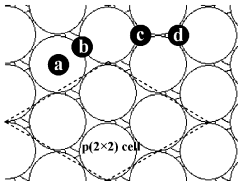

Figure 1. Top view of Ni(111): (a) top (tp) site, (b) bridge (br) site, (c) hexagonal-close-packed (hcp) site, and (d) face-centered cubic (fcc) site.

sequential total energy package (CASTEP).[32] Ionic cores were described by the ultrasoft pseudopotential,[33] and the Kohn−Sham one-electron states were expanded in a plane wave basis set up to 340 eV, which indicates that the atomic radius of 5 Å was considered in the integration calculation. A Fermi smearing of 0.1 eV was utilized. Brillouin zone integration was approximated by a sum over special *k* points ($5 \times 5 \times 1$) chosen using the Monhorst−Pack scheme.[34] The pseudopotential with partial core was used in spin-polarized calculations to include nonlinear core corrections[35] because spin polarization has major effects on the adsorption energies for a magnetic system.[36−40] The vacuum between the slabs was set to span a range of 12 Å to ensure no significant interaction between the slabs. The convergence criteria for structure optimization and energy calculation were set to (a) 1.0×10^{-6} eV/atom for SCF, (b) 1.0×10^{-5} eV/atom for energy, (c) 0.03 eV/Å for maximum force, and (d) 1.0×10^{-3} Å for maximum displacement. The bulk lattice constant was calculated to test the method and convergence criteria employed. The computed lattice constant (3.54 Å) with *k* points of $6 \times 6 \times 6$ agrees well with the experiment (3.52 Å), and this validates the employed methods and models nicely for nickel system.

The chemisorption energy of the intermediates (IM) is defined as $\Delta E_{chem} = E(\text{IM/slab}) - [E(\text{IM}) + E(\text{slab})]$, where E(IM/slab) is the total energy for the slab with the chemisorbed intermediates on the surface, E(IM) is the total energy of the free intermediates, and E(slab) is the total energy of the bare slab of the surface. Therefore, negative ΔE_{chem} means exothermic chemisorption, and positive ΔE_{chem} means endothermic chemisorption.

First, the three-layered models were used; afterward, the results were validated by using models with more layers. The computed structural and energetic parameters were compared between the three-layered models and the average of three-, four-, and five-layered ones. For the most stable chemisorption configurations on the surface, the differences in bond lengths and ΔE_{chem} are less than 0.001 Å and 0.01 eV, respectively. Therefore, the three-layered models were employed. In our calculations, the nickel atoms in the bottom were fixed in their bulk positions, while those in the top and second layers were allowed to relax (2Ni/1Ni). As shown in Figure 1, there are four surface sites on Ni(111): (a) top (tp) site, (b) bridge (br) site, (c) hexagonal close-packed (hcp) site, and (d) face-centered cubic (fcc) site. The $p(2 \times 2)$ unit cell was used to model the coverage of $^1/_4$ monolayer, as widely used in the previous theoretical investigations on the molecule chemisorptions on transition metal surfaces.[41−42] Test calculations showed no significant interaction between chemisorbed species at this coverage.[43]

The transition states (TS) were searched by using the complete LST/QST method.[44] First, the linear synchronous transit (LST) maximization was performed, followed by an energy minimization in directions conjugating to the reaction pathway. The approximated TS were used to perform quadratic synchronous transit (QST) maximization. From that point, another conjugate gradient minimization was performed. The cycle is repeated until a stationary point was located. The convergence criterion for the transition states search was set to 0.25 for the root mean square of atomic forces.

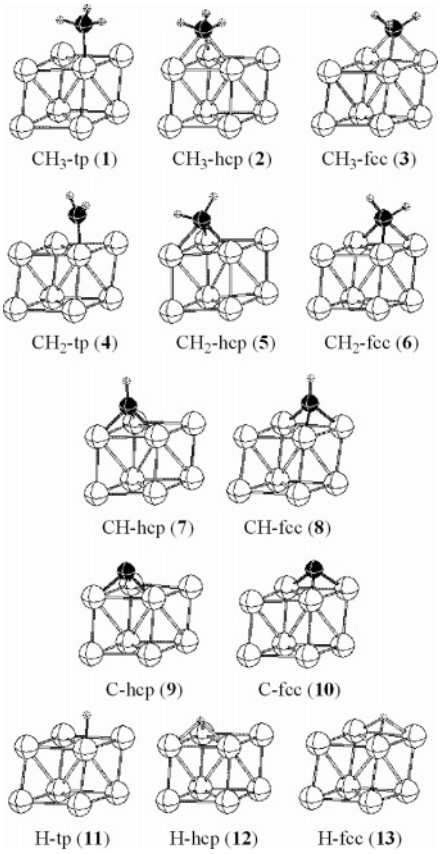

Figure 2. Optimized structures of chemisorbed CH_x species and H on Ni(111).

Results and Discussion

a. Chemisorbed CH_x Species. The calculation began with the CH_x species, which were widely studied experimentally[45−51] and theoretically[52−59] on other systems. The stable structures are shown in Figure 2, and the computed ΔE_{chem} are listed in Table 1.

On the top site, CH_3 interacts with one Ni atom, and the ΔE_{chem} of CH_3-tp (**1**) is −1.55 eV. For CH_3-hcp (**2**) and CH_3-fcc (**3**), CH_3 interacts with three Ni atoms, and the initial structure on the bridge site was optimized into CH_3-fcc (**3**). The ΔE_{chem} for **2** and **3** are −1.78 and −1.81 eV, respectively, and stronger than that for **1**. This indicates that CH_3 prefers chemisorbing on the 3-fold fcc and hcp sites of Ni(111).

For CH_2, three stable structures are obtained. In CH_2-tp (**4**), CH_2 interacts with one Ni atom, and the C−H bonds point to the vicinal Ni atoms, and the ΔE_{chem} for **4** is −2.78 eV. In CH_2-hcp (**5**) and CH_2-fcc (**6**), CH_2 interacts with three Ni atoms, and one of the C−H bonds points to the vicinal Ni atoms, while the initial structure on the bridge site was optimized into CH_2-fcc (**6**). The ΔE_{chem} for **5** and **6** are −3.83 and −3.85 eV, respectively, and more negative than that for **4**. Thus, CH_2 prefers chemisorbing on the 3-fold hcp and fcc sites on Ni(111).

For CH, only two stable structures are obtained, CH-hcp (**7**) and CH-fcc (**8**). CH interacts with three Ni atoms, and the orientation of C−H is vertical to Ni(111), while the initial structures on the top and bridge sites were optimized into CH-hcp (**7**). On both hcp (**7**) and fcc (**8**) sites, CH has a very negative ΔE_{chem} of −6.35 and −6.27 eV, respectively.

TABLE 1: Chemisorption Energies (ΔE_{chem}, eV), Charges (*q*, E), and Bond Lengths (*d*, Å) of CH_x and H Chemisorbed on Ni(111)

adsorbate	ΔE_{chem}	q	d_{C-H}
CH_3 (doublet)		0	1.081
CH_3-tp (**1**)	−1.55	−0.45	1.092, 1.092, 1.092
CH_3-hcp (**2**)	−1.78	−0.65	1.111, 1.111, 1.109
CH_3-fcc (**3**)	−1.81	−0.64	1.111, 1.111, 1.109
CH_2 (triplet)		0	1.078
CH_2-tp (**4**)	−2.78	−0.40	1.092, 1.094
CH_2-hcp (**5**)	−3.83	−0.64	1.096, 1.148
CH_2-fcc (**6**)	−3.85	−0.64	1.093, 1.144
CH (doublet)		0	1.123
CH-hcp (**7**)	−6.35	−0.52	1.094
CH-fcc (**8**)	−6.27	−0.50	1.093
C-hcp (**9**)	−6.61	−0.42	
C-fcc (**10**)	−6.52	−0.40	
H-tp (**11**)	−2.22 (−0.09[a])	−0.10	
H-hcp (**12**)	−2.76 (−0.99[a])	−0.26	
H-fcc (**13**)	−2.77 (−1.01[a])	−0.27	

[a] The chemisorption energies of H_2 dissociative chemisorption, $\Delta E_{chem}(H_2) = 2E(H/slab) - [E(H_2) + 2E(slab)]$.

Two stable structures are obtained for carbon atoms; however, no stable structures are found on the top and bridge sites. In C-hcp (**9**) and C-fcc (**10**), C interacts with three Ni atoms and forms three Ni−C bonds. The ΔE_{chem} for **9** and **10** are −6.61 and −6.52 eV, respectively.

For hydrogen atoms, three stable structures are found: H-tp (**11**), H-hcp (**12**), and H-fcc (**13**). Initial structure on the bridge site was optimized into the fcc site, and this disagrees with Kresse's result that hydrogen exists in the bridge site of Ni(111) at $^1/_4$ ML coverage.[60] The ΔE_{chem} relative to the hydrogen atom are −2.22, −2.76, and −2.77 eV for **11**, **12**, and **13**, respectively. Hydrogen prefers chemisorbing on the 3-fold hcp (**12**) and fcc (**13**) sites, in agreement with the previous theoretical results.[60,61] The ΔE_{chem} relative to H_2 dissociative chemisorption of H-hcp (**12**) and H-fcc (**13**) are −0.99 and −1.01 eV per H_2 (−22.8 and −23.3 kcal/mol), respectively, which are more close to the experimental value of 23 kcal/mol[61] than the previous theoretical result (−20.5 kcal/mol) by Watwe et al.[61]

As given in Table 1, CH_x and H prefers to chemisorb on the 3-fold hollow hcp and fcc sites on Ni(111), and both CH and atomic carbon have the strongest adsorption energies and, in turn, the highest stability toward desorption.

b. Chemisorbed Oxygenated Species. Experimental studies found CH_2O and CHO in steam reforming of CH_4.[62] In addition, no direct evidence was found to exclude to the possibilities of oxygenated species in CO_2 reforming of CH_4. In this part, our calculations on CH_xO and CH_xOH chemisorbed on Ni(111) are presented. The obtained stable structures are shown in Figures 3 and 4, and the computed ΔE_{chem} are listed in Tables 2 and 3, respectively.

In CO_2 reforming of CH_4, CO_2 dissociation on Ni forms chemisorbed O species. The potential reaction between O and CH_x can produce CH_xO species. Therefore, the structures and the ΔE_{chem} of CH_xO species are calculated in this part.

For CH_3O, two stable structures are found, CH_3O-hcp (**14**) and CH_3O-fcc (**15**), and three Ni−O bonds are formed. The ΔE_{chem} for **14** and **15** are −2.26 and −2.40 eV, respectively. However, no stable structures could be found on the top and bridge sites.

For CH_2O, four stable structures are obtained, and all of them have bent-down character, i.e., both oxygen and carbon atoms of CH_2O interact with surface Ni atoms. On the top site (**16**), oxygen and carbon interact with the same Ni atom on the surface, and the ΔE_{chem} is −0.33 eV. On the bridge site (**17**),

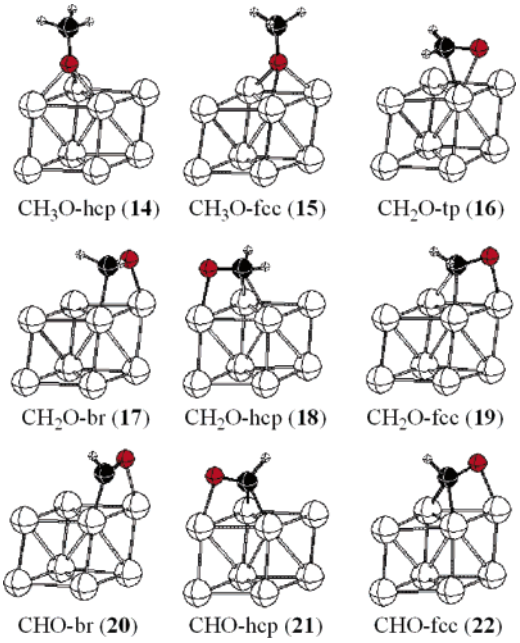

Figure 3. Optimized structures of chemisorbed CH_xO species on Ni(111).

one Ni−O and Ni−C bonds are formed, and the ΔE_{chem} is −0.53 eV. For CH_2O-hcp (**18**) and CH_2O-fcc (**19**), one Ni−O and two Ni−C bonds are formed, respectively. The ΔE_{chem} for **18** and **19** are −0.61 and −0.62 eV, respectively, and they indicate the weak stability toward desorption.

For CHO, three stable structures are obtained, and both oxygen and carbon atoms of CHO interact with the surface Ni atoms. In CHO-br (**20**), one Ni−O and one Ni−C bonds are formed. For CHO-hcp (**21**) and CHO-fcc (**22**), one Ni−O and two Ni−C bonds are formed in each case. As given in Table 2, the ΔE_{chem} for **20**, **21**, and **22** are −2.11, −2.25, and −2.24 eV, respectively. CHO prefers chemisorbing on the 3-fold hcp and fcc sites, but a small energetic difference between the chemisorbed states on the bridge site and 3-fold hollow site is found.

For all CH_xO species, CH_2O has rather small ΔE_{chem}, indicating that CH_2O is easy to desorb on Ni(111) once it forms. Comparatively, CH_3O and CHO have larger ΔE_{chem}.

Because both CH_xO hydrogenation and combination of CH_x and OH can produce CH_xOH, calculations on chemisorbed CH_xOH on Ni(111) were performed to analyze their possibilities in CO_2 reforming of CH_4.

As given in Figure 4 and Table 3, CH_3OH adsorbs on the top site (**23**) of Ni(111), and the ΔE_{chem} is only −0.07 eV. It indicates that CH_3OH adsorbs on Ni(111) very weakly.

CH_2OH can chemisorb on all of the four sites. On the top site (**24**), one Ni−C bond is formed, and the ΔE_{chem} is −1.36 eV. On the bridge site (**25**), one Ni−C and one Ni−C are formed, and the ΔE_{chem} is −1.40 eV. For CH_2OH-hcp (**26**) and CH_2OH-fcc (**27**), one Ni−O and two Ni−C bonds are formed, respectively. The ΔE_{chem} for **26** and **27** are −1.39 and −1.40 eV, respectively. It is noted that the ΔE_{chem} of CH_2OH on different sites are similar to each other, indicating the similar stability on these sites.

For CHOH, six stable structures are found. In gas phase, CHOH has a *trans*-CHOH structure (the dihedral angle of H−C−O−H is 180°), while that of *cis*-CHOH changes from 0° to 101°. In our calculations, *cis*-CHOH could exist on Ni(111), CHOH-tp-a (**28**), and CHOH-br-a (**30**), but they are less stable than their trans counterparts, CHOH-tp-b (**29**) and

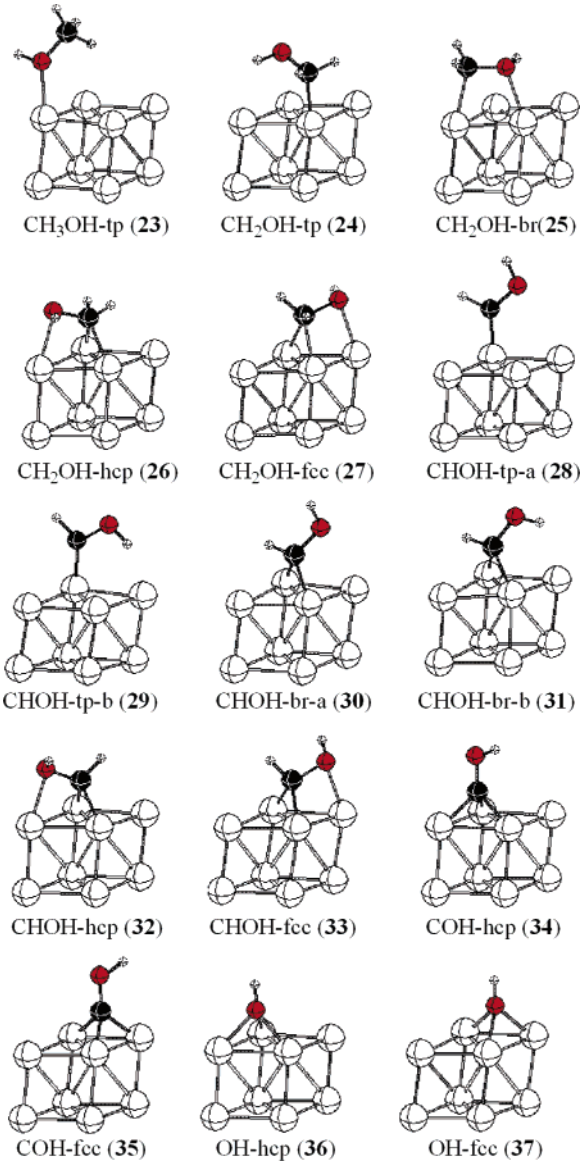

Figure 4. Optimized structures of chemisorbed CH_xOH species on Ni(111).

TABLE 2: Chemisorption Energies (ΔE_{chem}, eV), Charges (*q*, E), and Bond Lengths (*d*, Å) of CH_xO Chemisorbed on Ni(111)

adsorbate	ΔE_{chem}	q	d_{C-H}	d_{C-O}
CH_3O (doublet)		0	1.099, 1.103, 1.111	1.356
CH_3O-hcp (**14**)	−2.26	−0.44	1.094, 1.094, 1.094	1.421
CH_3O-fcc (**15**)	−2.40	−0.45	1.093, 1.094, 1.094	1.422
CH_2O (singlet)		0	1.107, 1.110	1.210
CH_2O-tp (**16**)	−0.33	−0.49	1.099, 1.099	1.293
CH_2O-br (**17**)	−0.53	−0.55	1.100, 1.102	1.333
CH_2O-hcp (**18**)	−0.61	−0.66	1.115, 1.130	1.322
CH_2O-fcc (**19**)	−0.62	−0.67	1.120, 1.122	1.321
CHO (doublet)		0	1.124	1.185
CHO-br (**20**)	−2.11	−0.38	1.106	1.249
CHO-hcp (**21**)	−2.25	−0.52	1.104	1.283
CHO-fcc (**22**)	−2.24	−0.52	1.104	1.281

CHOH-br-b (**31**). The ΔE_{chem} are −2.56 and −2.88 eV for **29** and **31**, respectively. For CHOH-hcp (**32**) and CHOH-fcc (**33**), one Ni−O and two Ni−C bonds are formed, and the dihedral angles of H−C−O−H are 57° and 51°, respectively. The ΔE_{chem} for **32** and **33** are −2.68 eV. It indicates that CHOH prefers chemisorbing on the bridge site.

TABLE 3: Chemisorption Energies (ΔE_{chem}, eV), Charges (*q*, E), and Bond Lengths (*d*, Å) of CH_xOH Chemisorbed on Ni(111)

adsorbate	ΔE_{chem}	q	d_{C-H}	d_{C-O}	d_{O-H}
CH_3OH (singlet)		0	1.090, 1.097, 1.098	1.418	0.971
CH_3OH-tp (**23**)	−0.07	−0.04	1.093, 1.095, 1.095	1.419	0.974
CH_2OH (doublet)		0	1.078, 1.082	1.361	0.973
CH_2OH-tp (**24**)	−1.36	−0.27	1.091, 1.096	1.395	0.978
CH_2OH-br (**25**)	−1.40	−0.32	1.091, 1.094	1.443	0.980
CH_2OH-hcp (**26**)	−1.39	−0.46	1.098, 1.115	1.445	0.981
CH_2OH-fcc (**27**)	−1.40	−0.47	1.098, 1.114	1.449	0.981
trans-CHOH (singlet)		0	1.116	1.308	0.982
CHOH-tp-a (**28**)	−2.25	−0.18	1.097	1.342	0.980
CHOH-tp-b (**29**)	−2.56	−0.12	1.096	1.317	0.998
CHOH-br-a (**30**)	−2.71	−0.38	1.102	1.379	0.977
CHOH-br-b (**31**)	−2.88	−0.31	1.102	1.353	0.987
CHOH-hcp (**32**)	−2.68	−0.42	1.099	0.431	0.980
CHOH-fcc (**33**)	−2.68	−0.43	1.099	1.426	0.980
COH (doublet)		0		1.266	1.004
COH-hcp (**34**)	−4.33	−0.30		1.329	0.981
COH-fcc (**35**)	−4.27	−0.29		1.328	0.981
OH (doublet)		0			0.986
OH-hcp (**36**)	−3.01	−0.35			0.974
OH-fcc (**37**)	−3.11	−0.35			0.973
H_2O (singlet)		0			0.972
H_2O-tp (**38**)	−0.05	0.04			0.973

For COH, two stable structures are found, COH-hcp (**34**) and COH-fcc (**35**). Three Ni−C bonds are formed, and the ΔE_{chem} for **34** and **35** are −4.33 and −4.27 eV, respectively. No bent-down adsorbed structures were found in our calculations.

OH prefers chemisorbing on the hcp (**36**) and fcc (**37**) sites, and the ΔE_{chem} are −3.01 and −3.11 eV, respectively. In addition, the adsorption of molecular H_2O is also calculated, and a very weakly adsorbed state is found on the top site (**38**), with ΔE_{chem} of only −0.05 eV.

c. Key Intermediates and Discussion. As shown in Figure 5, the thermodynamic scheme of CO_2 reforming of CH_4 on Ni(111) was derived from the ΔE_{chem}. The energies labeled in Figure 5 are the sum of the ΔE_{chem} of adsorbed species on their most stable sites relative to free CH_4 and CO_2.

The ΔE_{chem} of CO_2, CO, and O are taken from our previous study[43] by using the same method. CO_2 chemisorption on Ni(111) is slightly endothermic (0.31 eV), while its dissociation is strongly exothermic (−1.02 eV). Comparatively, CH_4 dissociative chemisorption is endothermic (0.16 eV).

Surface OH was proposed as the key intermediate to react with surface CH_x species by Walter et al.[63] However, many authors have claimed the adsorbed O atom to be the key intermediate.[64−66] Our calculation found surface O hydrogenation to surface OH to be endothermic (0.13 eV), indicating that surface OH has lower concentration than surface O on Ni(111). Because surface OH hydrogenation to H_2O needs more energy (0.50 eV), H_2O formation on Ni(111) is disfavored. Instead, H_2O dissociation is more favored than its formation. Compared to CO_2 dissociation, H_2O dissociation easily produces surface O, which in turn oxygenates surface carbon to CO. This is in agreement with the experimental results that steam reforming has less carbon deposition than CO_2 reforming, and addition of steam into CO_2 reforming of CH_4 reduces carbon deposition.[67,68] Furthermore, the reaction between surface OH and CH_3 is also strongly endothermic (0.60 eV), while the reaction between surface O and CH_3 needs only 0.22 eV. Thus, surface O rather than OH is the key intermediate and has higher reactivity with surface CH_x species.

In earlier investigations of catalytic mechanism of CO_2 reforming of CH_4, two dominating reaction pathways were proposed: $CH_4 \rightarrow CH_x \rightarrow C \rightarrow CO$ (CH_x pathway)[25,26] and

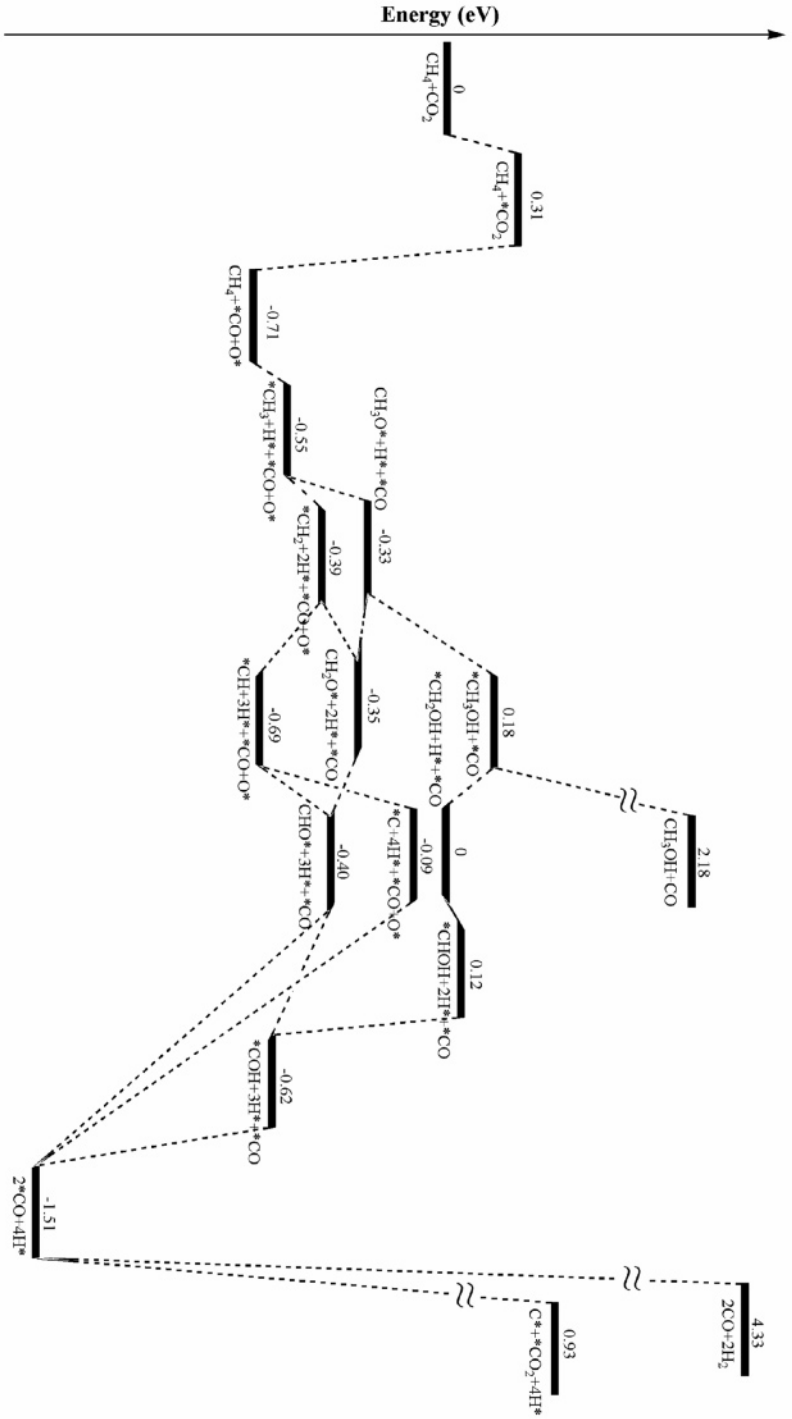

Figure 5. Thermodynamic scheme of CO_2 reforming of CH_4 on Ni(111).

$CH_4 \rightarrow CH_x \rightarrow CH_xO \rightarrow CO$ (CH_xO pathway).[27−29] Our previous investigation on thermal (noncatalytic) CO_2 reforming of CH_4 proposed the pathway of $CH_4 \rightarrow CH_3 \rightarrow CH_3O \rightarrow CH_2O \rightarrow CHO \rightarrow CO$.[69] However, which are the key intermediates along the reaction pathway on Ni-based catalysts?

Surface CH_3, from CH_4 dissociative chemisorption, has two possible reactions along the reaction pathways of CO_2 reforming of CH_4, i.e., oxygenation and dehydrogenation. CH_3 oxygenation to CH_3O needs 0.22 eV, while its dehydrogenation to CH_2 and H needs 0.16 eV. It indicates that CH_3 dehydrogenation is more favored than its oxygenation, but this small energetic difference cannot exclude the possibility of CH_3O formation. For surface CH_2, its dehydrogenation to CH and H is apparently exothermic (−0.30 eV), while its oxygenation to CH_2O needs 0.04 eV. Thus CH_2 prefers dehydrogenation to form CH. For CH_3O, its dehydrogenation to CH_2O is nearly thermally neutral (−0.02 eV), while its hydrogenation to CH_3OH needs more energy (0.51 eV). Comparatively, CH_2 has higher reactivity than CH_3O, and CH is the main intermediate in the next step. For CH, both its dehydrogenation and oxygenation are endothermic by 0.60 and 0.29 eV, respectively. By comparing the relative energies, CH oxygenation to CHO is favored. CHO dehydrogenation to CO and H is strongly exothermic (−1.11 eV) and favored strongly. Therefore, on the viewpoint of thermodynamics, the key intermediates of CO_2 reforming of CH_4 to produce CO and H_2 are CH_3, CH_2, CH, and CHO.

The reaction of CO_2 reforming of CH_4 to produce CO and H_2 is strongly endothermic (eq 3, 247 kJ/mol), which is larger

that that of formation of CH_3OH and CH_2O (eqs 4 and 5) in the gas phase.

$$CH_4 + CO_2 = CH_3OH + CO \qquad \Delta H^0_{298} = 74 \text{ kJ/mol} \tag{4}$$

$$CH_4 + CO_2 = 2CH_2O \qquad \Delta H^0_{298} = 60 \text{ kJ/mol} \tag{5}$$

However, CO and H_2 is more favored to form than CH_3OH and CH_2O thermodynamically on Ni(111), as shown in Figure 5. This can explain the high selectivity of synthesis gas in Ni-catalyzed CO_2 reforming of CH_4.

It is noted that CO is difficult to desorb from Ni(111) and needs 1.91 eV, although its formation is favored. Thus, CO is easy to accumulate on Ni(111). CO accumulation on the Ni surface may be one of the potential factors to restrain its further formation. In addition, CO accumulation promotes the Bouduard back reaction ($2CO = C_{(ads)} + CO_2$), which accelerates carbon deposition and, in turn, deactivates the catalysts. Therefore, it is proposed that the measures of promoting CO desorption could promote both CO selectivity and catalyst stability. For another key product H_2, its combinative desorption from Ni(111) needs 1.01 eV per molecular H_2. It is favored to form free H_2 in Ni-catalyzed CO_2 reforming of CH_4 compared to CO formation.

In previous studies, CH_4 dehydrogenation is proposed as another route of carbon deposition. In our calculation, CH is preferred to oxygenation to CHO, compared to its dehydrogenation, indicating that carbon deposition from CH_4 dehydrogenation is disfavored thermodynamically. Comparatively, Bouduard back reaction is promoted due to CO accumulation on the Ni surface and, therefore, the main reason for carbon deposition from the viewpoint of thermodynamics. However, under real reaction conditions, the feasibility of the oxygenation of CH to CHO depends on the concentration of surface oxygen produced by CO_2 dissociation, i.e., CH has to dehydrogenate to C and H in an oxygen-lacking environment (very high CH_4/CO_2 input ratio, $p(CH_4)/p(CO_2)$). Comparatively, high $p(CO)$ promotes the Bouduard back reaction to produce carbon deposition. This agrees with the experimental result[3] that the carbon formation rate increases with the increase of $p(CO)p(CH_4)/p(CO_2)$ value. In addition, the structures and energies in our paper were calculated at $^1/_4$ coverage, i.e., there is no significant interaction between chemisorbed species. Therefore, our results are suitable to compare with the experimental results under low pressure.

The energy barriers of the elementary steps of the most favorable reaction pathways were calculated to compare with the thermodynamic data; the optimized transition state structures by using the complete LST/QST method are shown in Figure 6. The adsorption energies of the coadsorbed species were compared with the sum of their individual adsorbed counterparts on their most favored sites.

As shown in Figure 6, the energy barrier of CH_4 (R1) dissociative adsorption is 1.18 eV, and that of its back reaction is 0.81 eV. The sum (−4.38 eV) of chemisorption energies of the coadsorbed CH_3 and H (P1) is slightly lower than that (−4.57 eV) of their individual adsorption energies. Further dehydrogenation of chemisorbed CH_3 (R2) to CH needs to overcome the energy barriers of 0.86 and 0.46 eV for each step, respectively. The energies of the coadsorbed CH_2 + H (P2), and CH + H (P3) are similar to the sum of their individual adsorbed counterparts. Therefore, the first dehydrogenation of CH_4 is kinetically more difficult than the subsequent two steps.

As shown in Figure 6, the lowest energy barrier of CH oxygenation to CHO is 0.89 eV (TS5). Comparatively, the dehydrogenation of CH to C has a high energy barrier (TS4, 1.47 eV), which is higher than the first step of CH_4 dehydrogenation. It indicates that the chemisorbed CH prefers to transfer to CHO under surface O existed environments kinetically. The chemisorption energy of the coadsorbed C + H (P4) is close to the sum of the individual adsorbed counterparts (−9.32 vs −9.38 eV). The chemisorption energy of the coadsorbed CH and O is −10.74 eV, which is 0.68 eV lower than the sum of their individual chemisorption (−11.42 eV). CHO (R6) dehydrogenation to CO and H also has a low energy barrier (0.32 eV).

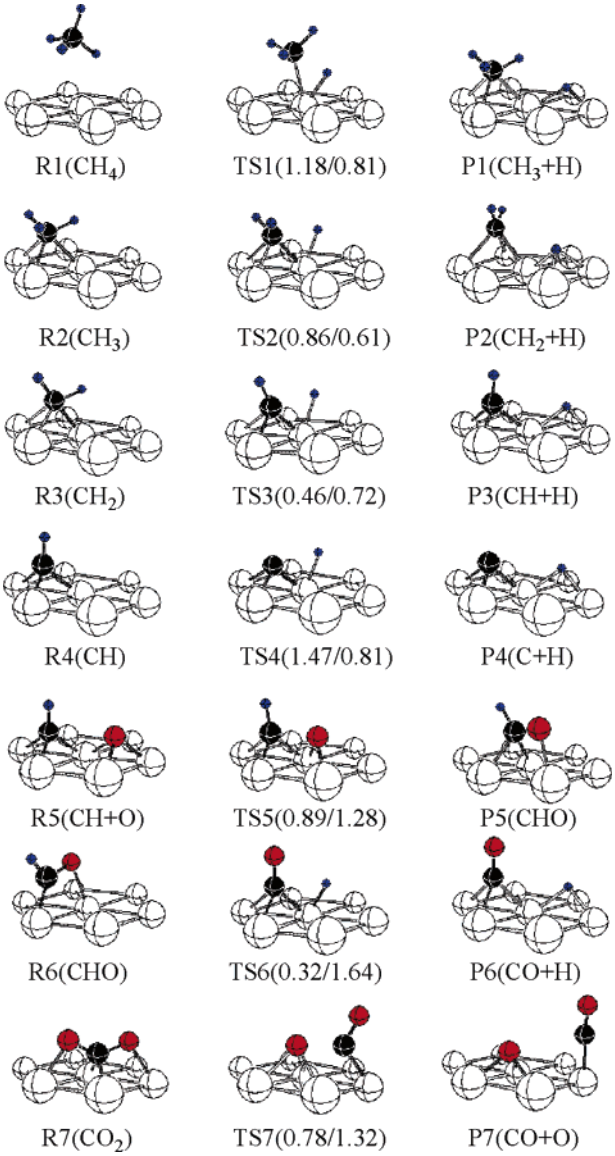

Figure 6. Optimized structures and reaction barriers (eV) of the transition states of the elementary steps in CO_2 reforming of CH_4 on Ni(111).

CO_2 dissociation on Ni(111) surface was calculated to compare with CH_4 activation. The lowest energy barrier is 0.78 eV, with the reaction mode in Figure 6 (R7 → TS7 → P7). This is 0.40 eV lower than that of CH_4 dissociation. Therefore, CH_4 dissociative adsorption is the most difficult step for the production of adsorbed CO.

On this basis, it is concluded that the rate-determining step of CH_4 conversion in the CO_2 reforming system is the first dehydrogenation of CH_4 with an energy barrier of 1.18 eV. This agrees with the previous kinetic assessment of the mechanism of CO_2 reforming of CH_4 by isotopic experiments;[3] the kinetic responses are consistent with rate-determining CH_4 activation

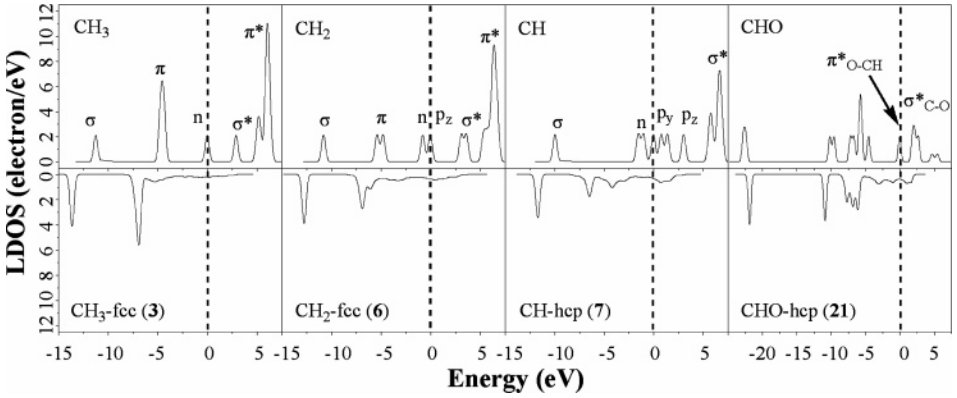

Figure 7. The LDOS of the key intermediates before and after chemisorption on Ni(111).

steps on a surface essentially free of reactive intermediates or coadsorbed products ($r_f = kp(CH_4)$). However, this barrier is lower than the desportion energy of CO (1.91 eV). Therefore, the effect of CO accumulation to the reaction is noticeable on both thermodynamics and kinetics.

d. Electronic Properties. From Tables 1−3, most of the surface species are negative charged after chemisorbing on Ni(111), except for surface H_2O (nearly neutral). It indicates significant electron transfer from Ni(111) to the intermediates upon chemisorption, which changes free CH_x, CH_xO, and CH_xOH to chemisorbed $CH_x^{\delta-}$, $CH_xO^{\delta-}$, and $CH_xOH^{\delta-}$ anions.

The local densities of states (LDOS) in Figure 7 are calculated to analyze the interaction between the surface and the key intermediates. For the ground states of free CH_3 and CH_2, the highest occupied molecular orbital (HOMO) has a *p* character, and the lowest unoccupied molecular orbital (LUMO) is the C−H antibonding orbital (σ^*). On Ni(111), both HOMO and LUMO interact with the surface Ni atoms, and the electrons transfer from the Ni surface to the C−H antibonding orbital (σ^*) of CH_3-fcc (**3**) and CH_2-fcc (**6**). Consequently, the C−H bonds of chemisorbed CH_3-fcc (**3**) and CH_2-fcc (**6**) are activated, and the orbital energies shift below the Fermi level after chemisorption. This is consistent with the C−H bonds elongation of CH_3 (1.081 to 1.111, 1.111 and 1.109 Å) and CH_2 (1.078 to 1.144 and 1.093 Å) after chemisorption. It is notable that the C−H bonds of chemisorbed CH_3-fcc (**3**) and CH_2-fcc (**6**) are longer than that of free CH_4 (1.089 Å), which means that C−H bonds of chemisorbed CH_3-fcc and CH_2-fcc is activated on Ni(111).

For CH, however, only the 2p orbitals of the carbon atom interact with the surface and receive electrons, while there is no electron transfer to the σ^*(C−H) antibonding orbital, which means no bond weakening. On the contrary, the electron transfer from the Ni surface to the 2p orbital of the C atom, which increased its negative charge, strengthens its attraction to the positively charged H, in turn strengthening the C−H bond. This is in agreement with the computed C−H bond shortening of chemisorbed CH-hcp (**7**) (1.123 to 1.094 Å) after chemisoption, compared to their free counterparts in the gas phase. Compared to molecular CH_4, the C−H bond of CH-hcp (**7**) is slightly activated. On Ni(111), CH-hcp (**7**) has a shorter C−H bond length than CH_3-fcc (**3**) and CH_2-fcc (**6**) (1.094 vs 1.111 and 1.144 Å). This is relative to the fact that CH_3 sequential dehydrogenation to CH, while CH is difficult to dehydrogenate to surface C, instead is easy to be oxygenated to CHO.

For free CHO, the HOMO is a half-filled π^*_{O-CH} orbital in the Fermi level. For the π^*_{O-CH} orbital, it has a bonding character between the H and the C atom, while it has an antibonding character between the O atom and the CH group. The LUMO of CHO is the π^*_{C-O} orbital. After chemisorption, electrons in the Ni surface transferred to the π^*_{O-CH} orbital. Consequently, the C−H bond is strengthened and the C−O bond is activated. From the LDOS of CHO-hcp (**21**), the π^*_{C-O} orbital also received electrons, and this also activated the C−O bond. The analyses of LDOS agrees with the computed result of the C−H bond shortening (1.124 to 1.104 Å) and the C−O bond elongation (1.185 to 1.283 Å) after chemisorption. Compared with CH-hcp (**7**), however, CHO-hcp (**21**) has a longer C−H bond (1.104 vs 1.094 Å), which means it is easier to dehydrogenate than CH-hcp (**7**). This is consistent with the conclusion, derived from the energetic analyses, that chemisorbed CH-hcp (**7**) prefers to be oxygenated to CHO-hcp (**21**), then CHO-hcp dehydrogenates to the main product CO and atomic H.

Conclusions

The thermodynamics of CO_2 reforming of CH_4 on Ni(111) has been investigated by using density functional theory calculation. The chemisorption structures of all possible intermediates were calculated on Ni(111), and the key intermediates were outlined according to the relative energies derived from their chemisorption energies. The activation mechanism of the key intermediates on Ni(111) is elucidated by the analyses of electron transfer, molecular orbital, and LDOS schemes.

On the basis of our thermodynamic analysis, O, CH_3, CH_2, CH, and CHO are the key intermediates. CH_4 is favored to dissociate to CH_3 ($CH_4 \rightarrow CH_3 + H$) and then transforms to CH by sequential dehydrogenation ($CH_3 \rightarrow CH_2 \rightarrow CH$). CH prefers to be oxygenated to CHO ($CH + O \rightarrow CHO$) rather than to be dehydrogenated ($CH \rightarrow C + H$). CHO dissociation to CO is strongly exothermic ($CHO \rightarrow CO + H$), therefore, it is favored. In addition, surface carbon formation by Bouduard back reaction ($2CO = C_{(ads)} + CO_2$) is found to be more favored than by CH_4 sequential dehydrogenation. Thus, Bouduard back reaction is the main reason for carbon deposition thermodynamically.

Although CO formation on Ni(111) is favored, its desorption to free CO needs high energy. This indicates that CO prefers to accumulate on the Ni catalyst surface. CO accumulation can hinder its yield and selectivity and accelerate the deactivation of catalysts. Thus, it is proposed that the measure of promoting CO desorption can promote performance of the Ni catalysts on the aspects of yield, selectivity, and conversion.

The general reaction of CO_2 reforming of CH_4 to produce CO and H_2 is strongly endothermic in the gas phase, but on the Ni(111) surface, the formation of CO and H_2 is more favored than that of CH_3OH and CH_2O. This can explain the higher selectivity toward the formation of CO and H_2 on Ni catalysts.

Finally the proposed CO_2 reforming of CH_4 on Ni(111) has the following steps: (i) CO_2 dissociation into CO and O ($CO_2 \rightarrow CO + O$), (ii) CH_4 sequential dissociation into CH ($CH_4 \rightarrow CH_3 \rightarrow CH_2 \rightarrow CH$), (iii) CH oxygenation into CHO ($CH + O \rightarrow CHO$), and (iv) CHO dissociation into CO and H ($CHO \rightarrow CO + H$).

On the basis of the computed energy barriers of the elementary steps along the most favorable reaction pathway, CH_4 activation into CH_3 and H is the rate-determining step of CO_2 reforming of CH_4 on the Ni(111) surface, in agreement with the isotopic experimental results. In addition, CH prefers oxygenation (CHO) rather than dissociation (C + H) both thermodynamically and kinetically.

Acknowledgment. This work was supported by Chinese Academy of Sciences and the National Nature Foundation of China (nos. 20473111 and 20590361).

Supporting Information Available: Total energies are given. This material is available free of charge via the Internet at hppt://pubs.acs.org.

References and Notes

(1) Hu, Y. H.; Ruckenstein, E. *Adv. Catal.* **2004**, *48*, 297.
(2) Rostrup-Nielsen, J. R.; Sehested, J.; Nørskov, J. K. *Adv. Catal.* **2002**, *47*, 65.
(3) Wen, J.; Iglesia, E. *J. Catal.* **2004**, *224*, 370.
(4) Wang, G.-C.; Zhou, Y.-H.; Morikawa, Y.; Nakamura, J.; Cai, Z.-S.; Zhao, X.-Z. *J. Phys. Chem. B* **2005,** *109*, 12431.
(5) Hu, Y. H.; Ruckenstein, E. *J. Phys. Chem. B* **1997**, *101*, 7563.
(6) Snoeck, J.-W.; Froment, G. F.; Fowles, M. *Ind. Eng. Chem. Res.* **2002**, *41*, 4252.
(7) Suzuki, K.; Wargadalam, V. J.; Onoe, K.; Yamaguchi, T. *Energy Fuels* **2001**, *15*, 571.
(8) Juan-Juan, J.; Román-Martínez, M. C.; Illán-Gómez, M. J. *Appl. Catal., A* **2004**, *264*, 169.
(9) Aartun, I.; Gjervan, T.; Venvik, H.; Görke, O.; Pfeifer, P.; Fathi, M.; Holmen, A.; Schubert, K. *Chem. Eng. J.* **2004**, *101*, 93.
(10) Wen, J.; Iglesia, E. *J. Phys. Chem. B* **2004**, *108*, 4094.
(11) Bradford, M. C. J.; Vannice, M. A. *Appl. Catal., A* **1996**, *142*, 73.
(12) Ahmed, K.; Foger, K. *Catal. Today* **2000**, *63*, 479.
(13) Wang, S.; Lu, G. *Energy Fuels* **1998**, *12*, 248.
(14) Aparico, L. M.; Ruiz, A. G.; Ramoa, I. R. *Appl. Catal., A* **1998**, *170*, 177.
(15) Tokunaga, O.; Ogasawara, S. *React. Kinet. Catal. Lett.* **1989**, *39*, 69.
(16) Horiuchi, T.; Sakuma, K.; Fukui, T.; Kubo, Y.; Osaki, T.; Mori, T. *Appl. Catal., A* **1996**, *144*, 111.
(17) Lemonidou, A. A.; Vasalos, L. A. *Appl. Catal., A* **2002**, *228*, 227.
(18) Ciobica, I. M.; Frechard, F.; van Santen, R. A.; Kleyn, A. W.; Hafner, J. *J. Phys. Chem. B* **2000**, *104*, 3364.
(19) Jansen, A. P. J.; Burghgraef, H. *Surf. Sci.* **1995**, *344*, 149.
(20) Yang, H.; Whitten, J. L. *J. Chem. Phys.* **1992**, *96*, 5529.
(21) Chorkendorff, I.; Alstruo, I.; Ullmann, S. *Surf. Sci.* **1990**, *227*, 291.
(22) Olgaard Nielsen, B.; Luntz, A. C.; Holmblad, P. M.; Chorkendorff, I. *Catal. Lett.* **1995**, *32*, 15.
(23) Beebe, T. P.; Goodman, D. W.; Kay, B. D.; Yates, J. T. *J. Chem. Phys.* **1987**, *87*, 2305.
(24) Jiang, X.; Goodman, D. W. *Catal. Lett.* **1990**, *4*, 173.
(25) Mark, M. F.; Maier, W. F. *Angew. Chem., Int. Ed. Engl.* **1994**, *33*, 1657.
(26) Lercher, J. A.; Bitter, J. H.; Hally, W.; Niessen, W.; Seshan, K. *Stud. Surf. Sci. Catal.* **1996**, *101*, 463.
(27) Bradford, M. C. J.; Vannice, M. A. *Appl. Catal., A* **1996**, *142*, 97.
(28) Bradford, M. C. J.; Vannice, M. A. *J. Catal.* **1998**, *173*, 157.
(29) Miller, J. A.; Bowman, C. T. *Prog. Energy Combust. Sci.* **1989**, *15*, 287.
(30) White, J. A.; Bird, D. M. *Phys. Rev. B* **1994**, *50*, 4954.
(31) Perdew, J. P.; Burke, K.; Ernzerhof, M. *Phys. Rev. Lett.* **1996**, *77*, 3865.
(32) (a) Payne, M. C.; Allan, D. C.; Arias, T. A.; Joannopoulos, J. D. *Rev. Mod. Phys.* **1992**, *64*, 1045. (b) Milman, V.; Winkler, B.; White, J. A.; Pickard, C. J.; Payne, M. C.; Akhmataskaya, E. V.; Nobes, R. H. *Int. J. Quantum Chem.* **2000**, *77*, 895.
(33) Vanderbilt, D. *Phys. Rev. B* **1990**, *41*, 7892.
(34) Monkhorst, H. J.; Pack, J. D. *Phys. Rev. B* **1976**, *13*, 5188.
(35) Louie, S. G.; Froyen, S.; Cohen, M. L. *Phys. Rev. B* **1982**, *26*, 1738.
(36) Nayak, S. K.; Nooijen, M.; Bernasek, S. L. *J. Phys. Chem. B* **2001**, *105*, 164.
(37) Cheng, H. S.; Reiser, D. B.; Dean, S. W., Jr.; Baumert, K. *J. Phys. Chem. B* **2001**, *105*, 12547.
(38) Ge, Q.; Jenkins, S. J.; King, D. A. *Chem. Phys. Lett.* **2000**, *327*, 125.
(39) Ge, Q.; Neurock, M.; Wright, H. A.; Srinivasan, N. *J. Phys. Chem. B* **2002**, *106*, 2826.
(40) Cao, D.-B.; Zhang, F.-Q.; Li, Y.-W.; Jiao, H. *J. Phys. Chem. B* **2004**, *108*, 9094.
(41) Bengaard, H. S.; Alstrup, I.; Chorkendorff, I.; Ullmann, S.; Rostrup-Nielsen, J. R. *J. Catal.* **1999**, *187*, 238.
(42) Ledentu, V.; Dong, W.; Sautet, P. *J. Am. Chem. Soc.* **2000**, *122*, 1796.
(43) Wang, S.-G.; Cao, D.-B.; Li, Y.-W.; Wang, J.; Jiao, H. *J. Phys. Chem. B* **2005**, *109*, 18956.
(44) Halgren, T. A.; Lipscomb, W. N. *Chem. Phys. Lett.* **1977**, *49*, 225.
(45) Kaminsky, M. P.; Winograd, N.; Geoffroy, G. L.; Vannice, M. A. *J. Am. Chem. Soc.* **1986**, *108*, 1315.
(46) Yang, Q. Y.; Maynard, K. J.; Johnson, A. D.; Ceyer, S. T. *J. Chem. Phys.* **1995**, *102*, 7734.
(47) Schouten, F. C.; Kaleveld, E. W.; Bootsma, G. A. *Surf. Sci.* **1977**, *63*, 460.
(48) Schouten, F. C.; Gijzeman, O. L. J.; Bootsma, G. A. *Bull. Soc. Chim. Belg.* **1979**, *88*, 541.
(49) Schouten, F. C.; Gijzeman, O. L. J.; Bootsma, G. A. *Surf. Sci.* **1979**, *87*, 1.
(50) Abbott, H. L.; Bukoski, A.; Kavulak, D. F.; Harrison, I. *J. Chem. Phys.* **2003**, *119*, 6407.
(51) Guo, H.; Zaera, F. *J. Phys. Chem. B* **2004**, *108*, 16220.
(52) Watwe, R. M.; Bengaard, H. S.; Rostrup-Nielsen, J. R.; Dumesic, J. A.; Nørskov, J. K. *J. Catal.* **2000**, *189*, 16.
(53) Yang, H.; Whitten, J. L. *J. Am. Chem. Soc.* **1991**, *113*, 6442.
(54) Yang, H.; Whitten, J. L. *J. Chem. Phys.* **1989**, *91*, 126.
(55) Kratzer, P.; Hammer, B.; Nørskov, J. K. *J. Chem. Phys.* **1996**, *105*, 5595.
(56) Swang, O.; Faegri, K., Jr.; Gropen, O.; Wahlgren, U.; Siegbahn, P. *Chem. Phys.* **1991**, *156*, 379.
(57) Siegbahn, P. E. M.; Panas, I. *Surf. Sci.* **1990**, *240*, 37.
(58) Lee, M. B.; Yang, Q. Y.; Ceyer, S. T. *J. Chem. Phys.* **1987**, *87*, 2724.
(59) Lee, M. B.; Yang, Q. Y.; Tang, S. L.; Ceyer, S. T. *J. Chem. Phys.* **1986**, *85*, 1693.
(60) Kresse, G.; Hafner, J. *Surf. Sci.* **2000**, *459*, 287.
(61) Christmann, K.; Schober, O.; Ertl, G.; Neumann, M. *J. Chem. Phys.* **1974**, *60*, 4528.
(62) Menon, P. G.; de Deken, J. C.; Froment, G. F. *J. Catal.* **1985**, *95*, 313.
(63) Walter, K.; Buyevskaya, O. V.; Wolf, D.; Baerns, M. *Catal. Lett.* **1994**, *29*, 261.
(64) Qin, D.; Lapszewicz, J.; Jiang, X. *J. Catal.* **1996**, *159*, 140.
(65) Shustorovich, E. *Adv. Catal.* **1990**, *37*, 101.
(66) Shustorovich, E.; Bell, A. T. *Surf. Sci.* **1991**, *248*, 359.
(67) Choudhary, V. R.; Rajput, A. M.; Prabhakar, B. *Angew. Chem., Int. Ed. Engl.* **1994**, *33*, 2104.
(68) Choudhary, V. R.; Uphade, B. S.; Mamman, A. S. *Appl. Catal., A* **1998**, *168*, 33.
(69) Wang, S.-G.; Li, Y.-W.; Lu, J.-X.; He, M.-Y.; Jiao, H. *J. Mol. Struct. (THEOCHEM)* **2004**, *673*, 181.